

Controlled Acidolysis of Hexacarbonyltris(μ -alkoxo)dirhenium(I) Anions: Facile Synthesis of Hexacarbonylbis(μ -alkoxo)- $[\mu$ -1,1'-bis(diphenylphosphino)ferrocene]dirhenium(I) Complexes and Nonacarbonyltris(μ -methoxo)(μ_3 -methoxo)trirhenium(I)

Chenghua Jiang,[†] Yuh-Sheng Wen,[‡] Ling-Kang Liu,^{*,‡} T. S. Andy Hor,^{*,†} and Yaw Kai Yan^{*,§}

Department of Chemistry, Faculty of Science, National University of Singapore, Kent Ridge, Singapore 119260, Institute of Chemistry, Academia Sinica, Taipei, Taiwan 11529, and Division of Chemistry, National Institute of Education, Nanyang Technological University, 469 Bukit Timah Road, Singapore 259756

Received July 18, 1997[®]

The complexes $[\text{Re}_2(\mu\text{-OR})_2(\mu\text{-dppf})(\text{CO})_6]$ (R = H, **1**; Me, **2**; Et, **3**; Ph, **4**) were synthesized by the controlled acidolysis of the anions $[\text{Re}_2(\mu\text{-OR})_3(\text{CO})_6]^-$ (R = H, Me, Et) and $[\text{Re}_2(\mu\text{-OH})(\mu\text{-OPh})_2(\text{CO})_6]^-$ (**5**), respectively, in the presence of dppf (1,1'-bis(diphenylphosphino)ferrocene). The dppf ligands in complexes **1–4** undergo a twisting motion in solution at room temperature, which, in the case of **3**, is correlated with the restricted rotation of the ethyl groups about the O–CH₂ bonds. Complex **3** is an interesting example of an organometallic complex in which the two exchanging positions of the methylene protons of an ethyl group are nonequivalent, while the exchanging positions of the methyl group are equivalent. Controlled acidolysis of $[\text{Re}_2(\mu\text{-OMe})_3(\text{CO})_6]^-$ under 1 atm of CO pressure affords the complex $[\text{Re}_3(\mu\text{-OMe})_3(\mu_3\text{-OMe})(\text{CO})_9]^-$ (**6**), which consists of a Re₃ triangle held together by one face-capping and three bridging methoxo groups, with no Re–Re bonds. The crystal structures of **1**, **3**, **5**, and **6** were determined by single-crystal X-ray diffraction analysis. The synthetic relationship of dirhenium–dialkoxo, dirhenium–trialkoxo, and trirhenium–tetraalkoxo entities is established.

Introduction

The synthesis, reactions, and solution dynamics of rhenium(I) carbonyl alkoxo complexes is a subject of current interest.¹ Much of our attention had been focused on the diphosphine- and dimethoxo-bridged complexes $[\text{Re}_2(\mu\text{-OMe})_2(\mu\text{-PP})(\text{CO})_6]$ {PP = dppf [1,1'-bis(diphenylphosphino)ferrocene] Ph₂P(CH₂)_nPPh₂, n = 1–4), which were synthesized by the oxidative decarbonylation of Re₂(CO)₁₀ by Me₃NO in a mixture of THF and MeOH, followed by the addition of diphosphine.^{1b,c} Curiously, this synthetic route cannot be extended to the synthesis of the analogous complexes $[\text{Re}_2(\mu\text{-OR})_2(\mu\text{-PP})(\text{CO})_6]$ (R = H, Et, Ph, CH₂CH₂Cl).^{1a,d} It is also

noteworthy that while the complexes $[\text{Re}_2(\mu\text{-OH})_2(\mu\text{-PP})(\text{CO})_6]$ (PP = dppm, dmpm, dppe, dmpe)² have been synthesized by the photolysis of $[\text{Re}_2(\mu\text{-PP})(\text{CO})_8]$ in wet toluene,³ the OEt, OPh, and OCH₂CH₂Cl analogues have not been reported.

It is somewhat surprising that to date there is no synthetic relationship between the bis(alkoxo)-bridged complexes $[\text{Re}_2(\mu\text{-OR})_2(\mu\text{-PP})(\text{CO})_6]$ and the well-established tris(alkoxo)-bridged complexes $[\text{Re}_2(\mu\text{-OR})_3(\text{CO})_6]^-$.^{4,5} In this paper, we report the facile synthesis of the complexes $[\text{Re}_2(\mu\text{-OR})_2(\mu\text{-dppf})(\text{CO})_6]$ (R = H, **1**; Me, **2**; Et, **3**; Ph, **4**) by the controlled acidolysis of the complexes $[\text{Re}_2(\mu\text{-OH})(\mu\text{-OPh})_2(\text{CO})_6]^-$ (**5**) and $[\text{Re}_2(\mu\text{-OR})_3(\text{CO})_6]^-$ (R = H, Me, Et) in the presence of dppf (Scheme 1). In order to investigate the stereogeometrical effects of the hydroxide and alkoxide ligands on the

[†] National University of Singapore.

[‡] Academia Sinica.

[§] Nanyang Technological University.

[®] Abstract published in *Advance ACS Abstracts*, December 15, 1997.

(1) (a) Jiang, C. H.; Wen, Y.-S.; Liu, L.-K.; Hor, T. S. A.; Yan, Y. K. *J. Organomet. Chem.* **1997**, *543*, 179. (b) Yan, Y. K.; Chan, H. S. O.; Hor, T. S. A.; Tan, K. L.; Liu, L.-K.; Wen, Y.-S. *J. Chem. Soc., Dalton Trans.* **1992**, 423. (c) Low, P. M. N.; Yong, Y. L.; Yan, Y. K.; Hor, T. S. A.; Lam, S.-L.; Chan, K. K.; Wu, C.; Au-Yeung, S. C. F.; Wen, Y.-S.; Liu, L.-K. *Organometallics* **1996**, *15*, 1369. (d) Hor, T. S. A.; Lam, C. F.; Yan, Y. K. *Bull. Singapore Natl. Inst. Chem.* **1991**, *19*, 115. (e) Mandal, S. K.; Ho, D. M.; Orchin, M. *Organometallics* **1993**, *12*, 1714. (f) Mandal, S. K.; Ho, D. M.; Orchin, M. *Inorg. Chem.* **1991**, *30*, 2244. (g) Herrmann, W. A.; Egli, A.; Herdtweck, E.; Alberto, R.; Baumgärtner, F. *Angew. Chem., Int. Ed. Engl.* **1996**, *35*, 432.

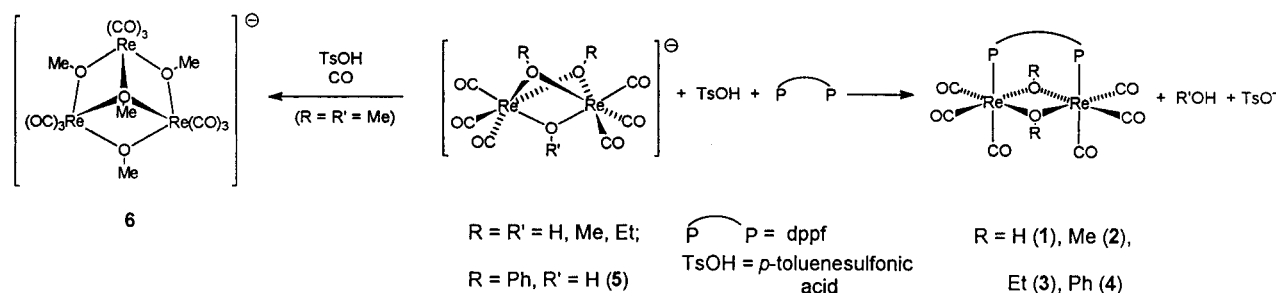
(2) Abbreviations used: dppm = bis(diphenylphosphino)methane, dmpm = bis(dimethylphosphino)methane, dppe = 1,2-bis(diphenylphosphino)ethane, dmpe = 1,2-bis(dimethylphosphino)ethane.

(3) Lee, K.-W.; Pennington, W. T.; Cordes, A. W.; Brown, T. L. *Organometallics* **1984**, *3*, 404.

(4) Ioganson, A. A.; Lokshin, B. V.; Kolobova, E. E.; Anisimov, K. N. *J. Gen. Chem.* **1974**, *20*, 20. (Translated from *Zh. Obshch. Khim.* **1974**, *44*, 23.)

(5) (a) Ginsberg, A. P.; Hawkes, M. J. *J. Am. Chem. Soc.* **1968**, *90*, 5930. (b) Ciani, G.; D'Alfonso, G.; Freni, M.; Romiti, P.; Sironi, A. *J. Organomet. Chem.* **1978**, *152*, 85. (c) Freni, M.; Romiti, P. *Atti Accad. Naz. Lincei, Mem. Cl. Sci. Fis. Mat. Nat. Rend.* **1973**, *55*, 515.

Scheme 1



dirhenium core, the variable-temperature ^1H NMR behavior of **3** was studied and the crystal structures of **1** and **3** determined and compared with that of **2**.^{1b} We also report the crystal structures of **5** and $[\text{NET}_4][\text{Re}_3(\mu\text{-OMe})_3(\mu_3\text{-OMe})(\text{CO})_9]$ (**6**), the latter of which was obtained from the acidolysis of $[\text{Re}_2(\mu\text{-OMe})_3(\text{CO})_6]^-$ under 1 atm of CO gas. The structure of **5** would reveal any structural deformities imposed by the mixed alkoxide ligands, while that of **6** provides a direct comparison of a Re_3 with the Re_2 entities.

Results and Discussion

Synthesis of the Dirhenium Anions $[\text{Re}_2(\mu\text{-OR})_3(\text{CO})_6]^-$ ($\text{R} = \text{H}, \text{Me}, \text{Et}$) and $[\text{Re}_2(\mu\text{-OH})(\mu\text{-OPh})_2(\text{CO})_6]^-$. The tris(alkoxo)-bridged complexes $[\text{Re}_2(\mu\text{-OR})_3(\text{CO})_6]^-$ ($\text{R} = \text{H}, \text{Me}, \text{Et}$) are easily synthesized by the reaction of $\text{ReBr}(\text{CO})_5$ with the corresponding base, NaOR, in a mixture of THF and ROH at room temperature. We found this method more convenient than those involving refluxing conditions using $\text{ReBr}(\text{CO})_5$ or $\text{Re}_2(\text{CO})_{10}$ in alcoholic solutions of NaOR or KOH.^{4,5} Surprisingly, the complex $[\text{Re}_2(\mu\text{-OPh})_3(\text{CO})_6]^-$ was not obtained in the analogous reaction with NaOPh under anhydrous conditions. A complex mixture of numerous products was obtained instead. When wet THF ($[\text{H}_2\text{O}]:[\text{ReBr}(\text{CO})_5]:[\text{OPh}^-]$ ca. 1:2:6) was used as the solvent, however, the novel mixed-bridge complex $[\text{Re}_2(\mu\text{-OH})(\mu\text{-OPh})_2(\text{CO})_6]^-$ (**5**) was obtained in good yield. Increasing the water content of the reaction mixture ($[\text{H}_2\text{O}]:[\text{ReBr}(\text{CO})_5]:[\text{OPh}^-]$ ca. 5:1:3) resulted in the formation of $[\text{Re}_2(\mu\text{-OH})_3(\text{CO})_6]^-$ as the main product.

Crystal Structure of $[\text{NET}_4][\text{Re}_2(\mu\text{-OH})(\mu\text{-OPh})_2(\text{CO})_6]^-$ (5**).** The molecular structure of the complex anion (Figure 1) consists of two $[\text{Re}(\text{CO})_3]$ fragments bridged by two OPh^- ligands and one OH^- ligand. To our knowledge, complex **5** is the first structurally well-defined mixed-bridge $[\text{Re}_2(\mu\text{-OR})_x(\mu\text{-OR}')_y(\text{CO})_6]^-$ ($x + y = 3$) complex that is synthesized in good yield.⁶ There have been two reports of the X-ray diffraction analysis of the complexes $[\text{Re}_2(\mu\text{-OMe})_x(\mu\text{-OEt})_y(\text{CO})_6]^-$ ($x + y = 3$).⁷ In these cases, complete formulation of the com-

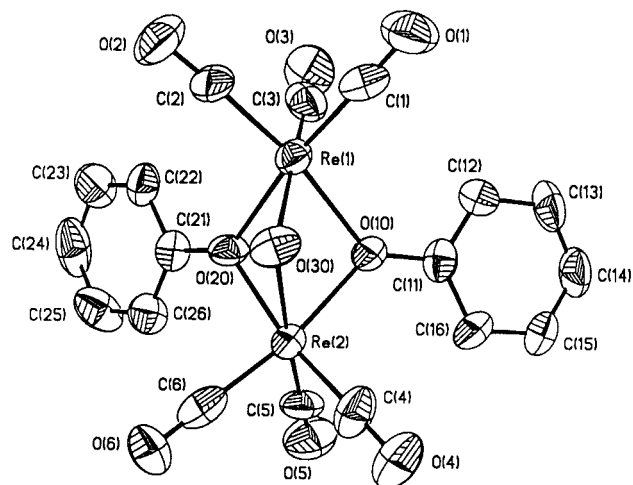


Figure 1. Crystal structure of $[\text{Re}_2(\mu\text{-OH})(\mu\text{-OPh})_2(\text{CO})_6]^-$ (**5**; 50% probability ellipsoids).

plexes was not successful due to the severe disorder of the alkoxo ligands.

The Re atoms in **5** exhibit a distorted octahedral geometry and fulfill the 18-electron rule without the need for a direct metal-metal bond. The $\text{Re}\cdots\text{Re}$ nonbonding distance of 3.152 Å is essentially identical to that in $[\text{Re}_2(\mu\text{-OPh})_3(\text{CO})_6]^-$ (3.154 Å).^{6c} The $\text{Re}(\mu\text{-O})\text{-Re}$ bond angles for the OPh^- ligands ($93.6(3)^\circ$ and $94.3(3)^\circ$) are somewhat smaller than that for the OH^- bridge ($95.5(4)^\circ$). This corresponds to a longer average $\text{Re}-\text{O}(\text{Ph})$ bond length (2.156(8) Å) compared to the average $\text{Re}-\text{O}(\text{H})$ bond length (2.128(9) Å). Comparable bond lengths and angles have been observed in $[\text{Re}_2(\mu\text{-OPh})_3(\text{CO})_6]^-$ and $[\text{Re}_2(\mu\text{-OH})_3(\text{CO})_6]^-$.^{6a,c} The $\text{Re}-\text{CO}$ bond lengths are identical within experimental error. The weaker $\text{Re}-\text{O}(\text{Ph})$ bonds are consistent with the experimental observation that the formation of the trihydroxo or mixed-ligand hydroxo/phenoxo complex is favored over that of the triphenoxo complex.

Synthesis and Characterization of $[\text{Re}_2(\mu\text{-OR})_2(\mu\text{-dppf})(\text{CO})_6]^-$ ($\text{R} = \text{H}, \mathbf{1}; \text{Me}, \mathbf{2}; \text{Et}, \mathbf{3}; \text{Ph}, \mathbf{4}$). Complexes **1–4** were synthesized by the stoichiometric protonation of $[\text{Re}_2(\mu\text{-OR})_3(\text{CO})_6]^-$ ($\text{R} = \text{H}, \text{Me}, \text{Et}$) and $[\text{Re}_2(\mu\text{-OH})(\mu\text{-OPh})_2(\text{CO})_6]^-$ (**5**), respectively, by *p*-toluenesulfonic acid (TsOH), followed by attack of dpfp (Scheme 1). In all cases, it was possible to selectively replace one of the bridging OR^- groups with the diphosphine. It is also noteworthy that in **5** the OH^- group is preferentially substituted over the bulkier OPh^- groups. This may be attributed to the higher basicity of the hydroxide, which renders it more susceptible to acid attack.

(6) Well-refined crystal structures have been reported for the following homobridged $[\text{Re}_2(\mu\text{-OR})_3(\text{CO})_6]^-$ complexes: (a) $\text{R} = \text{H}$. Alberto, R.; Egli, A.; Abram, U.; Hegetschweiler, K.; Gramlich, V.; Schubiger, P. A. *J. Chem. Soc., Dalton Trans.* **1994**, 2815. (b) $\text{R} = \text{Me}$. Herrmann, W. A.; Mihailos, D.; Ófele, K.; Kiprof, P.; Belmedjahed, F. *Chem. Ber.* **1992**, 125, 1795. (c) $\text{R} = \text{Ph}$. Beringhelli, T.; Ciani, G.; D'Alfonso, G.; Sironi, A.; Freni, M. *J. Chem. Soc., Dalton Trans.* **1985**, 1507.

(7) (a) Kolobova, N. E.; Zdanovich, V. I.; Lobanova, I. A.; Andrianov, V. G.; Struchkov, Yu. T.; Petrovskii, P. V. *Bull. Acad. Sci. USSR, Div. Chem. Sci.* **1984**, 33, 871. (b) Ciani, G.; Sironi, A.; Albinati, A. *Gazz. Chim. Ital.* **1979**, 109, 615.

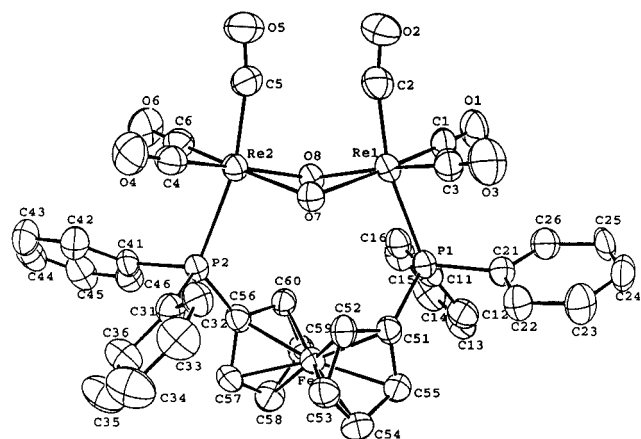


Figure 2. Crystal structure of $\text{Re}_2(\mu\text{-OH})_2(\mu\text{-dppf})(\text{CO})_6$ (**1**; 50% probability ellipsoids).

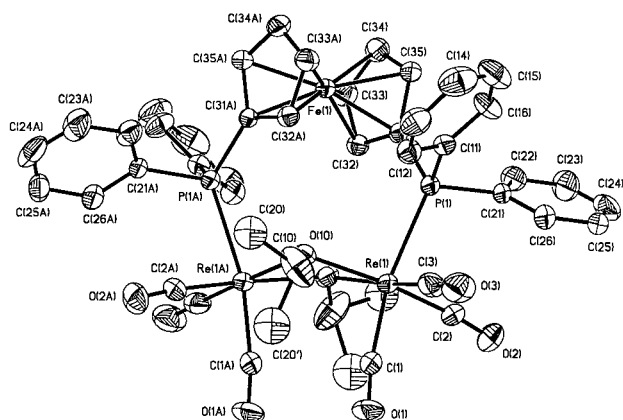


Figure 3. Crystal structure of $\text{Re}_2(\mu\text{-OEt})_2(\mu\text{-dppf})(\text{CO})_6$ (**3**; 30% probability ellipsoids).

While **1** was obtained in high yield from the acidolysis reaction carried out in THF, the yield of **2** was very low in THF. Infrared spectroscopy indicated that the predominant species present in the latter reaction mixture were probably $\text{fac-}[\text{ReX}(\text{CO})_3(\eta^2\text{-dppf})]^{n+}$ complexes ($X = \text{OTs}$ ($n = 0$) or THF ($n = 1$)). The yield of **2** increased dramatically when a mixture of CHCl_3 and MeOH was used as the solvent for the acidolysis reaction.

A mixture of chloroform and ethanol was used as the solvent for the synthesis of complex **3**. The yield of this complex was, however, significantly lower than those for **1** and **2**. This is probably due to the bulkiness of the OEt^- group, which hinders both the approach of the acid molecules and the coordination of dppf.

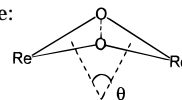
Crystal Structures of 1 and 3. The crystal structures of **1** and **3** are depicted in Figures 2 and 3, respectively. Complex **3** possesses a crystallographic C_2 axis (passing through the Fe atom and the center of the $\{\text{Re}_2\text{O}_2\}$ core), so that only half of the molecule is unique. Both **1** and **3** are structurally similar to **2**,^{1b} with dppf and two OR^- ligands bridging two *facial* $\text{Re}(\text{I})$ tricarbonyl moieties. The bulk of the dppf bridge forces the $\text{Cp}\cdots\text{Cp}$ axis⁸ to twist significantly with respect to the $\text{Re}\cdots\text{Re}$ axis and the two Re coordination planes to fold along the $\text{O}\cdots\text{O}$ axis away from the diphosphine. A comparison of selected structural parameters of complexes **1–3** is provided in Table 1.

(8) In this paper, Cp is used as the abbreviation for the substituted cyclopentadienyl ring, C_5H_4 , rather than the conventional C_5H_5 .

Table 1. Comparison of Selected Structural Parameters of $[\text{Re}_2(\mu\text{-OR})_2(\mu\text{-dppf})(\text{CO})_6]$ ($\text{R} = \text{H}$, **1**; Me , **2**; Et , **3**)

complex	$\text{Re}\cdots\text{Re}$ distance (Å)	θ (deg) ^a	average $\angle(\text{O}-\text{Re}-\text{O})$ in $\{\text{Re}_2\text{O}_2\}$ core (deg)	ω (deg) ^b	ϕ (deg) ^c	α (deg) ^d
1	3.42	29.7	70.7(2)	86.1	46.1	121.8
2	3.40	30.7	71.3(2)	85.9	53.5	122.6
3	3.43	26.3	72.8(3)	84.0	50.8	123.7

^a θ is the fold angle of the $\{\text{Re}_2\text{O}_2\}$ core:



^b ω is the angle by which the two Cp rings of the dppf ligand are twisted from the P, P eclipsed position. ^c ϕ is the angle made by the projection of the $\text{Cp}\cdots\text{Cp}$ axis of dppf onto the $\text{Re}\cdots\text{Re}$ axis. ^d α is the average $\text{C}_{\text{ipso}(\text{Cp})}-\text{P}-\text{Re}$ angle.

The ability of the dppf ligand to fine-tune its conformation to adjust to the steric demands of its molecular environment is reflected by the variation in the structural parameters listed in Table 1. The parameter that is most sensitive seems to be the angle (ϕ) made by the projection of the $\text{Cp}\cdots\text{Cp}$ axis of dppf onto the $\text{Re}\cdots\text{Re}$ axis. It is also evident that the fold angle θ of the $\{\text{Re}_2\text{O}_2\}$ core for the ethoxo complex **3** is significantly smaller than those of complexes **1** and **2**. The variations in θ and ϕ are, however, not monotonic with the steric bulk of the alkoxo bridges. On the other hand, the strain on the $\text{C}_{\text{ipso}(\text{Cp})}-\text{P}-\text{Re}$ angle appears to increase with increasing bulk of the alkoxo groups.

There is a disorder of the methyl groups of the ethoxo ligands in **3**, as shown in Figure 3. The structure was refined with two positions for the methyl carbon ($\text{C}(20)$ and $\text{C}(20')$) having occupancies of 60% and 40%, respectively. Both positions are directed away from the phenyl ring ($\text{C}(11)-\text{C}(16)$).

¹H NMR Spectroscopic Studies. The Cp resonances in the room temperature ^1H NMR spectra of **1**, **3**, and **4** comprise two extremely broad signals in the region 5.5–3.5 ppm. This pattern is very similar to that observed in the room temperature ^1H NMR spectrum of **2**, which has been interpreted in terms of an exchange of Cp protons due to the twisting motion of the bridging dppf ligand with respect to the axis joining the two bridged Re atoms.⁹

An interesting feature of the ^1H NMR spectrum of complex **3** (Figure 4a) is that the signal due to the methylene protons of the ethyl group takes the form of a broad singlet (at 4.65 ppm) instead of the familiar quartet, suggesting fluxionality involving the methylene protons. The signal for the CH_3 groups is, however, in the expected form of a triplet at 1.45 ppm. The ^1H NMR spectrum recorded at 243 K (Figure 4b) shows two well-resolved quartets¹⁰ attributable to the methylene protons at 4.44 and 4.86 ppm. At this temperature, the Cp signals are also resolved into four sharp singlets at 3.00, 3.88, 4.19 and 5.74 ppm. These Cp ^1H chemical shifts are very close to those observed for **2** at 228 K, for which the large range of chemical shifts has been

(9) Lam, S.-L.; Cui, Y.-X.; Au-Yeung, S. C. F.; Yan, Y.-K.; Hor, T. S. *A. Inorg. Chem.* **1994**, *33*, 2407.

(10) The term "quartets" is used here since the methylene proton signals resemble the 1:3:3:1 quartet expected in the first-order ^1H NMR spectrum of an ethyl group. The methylene signals observed here are not first order, however, as discussed in the subsequent paragraph of the text.

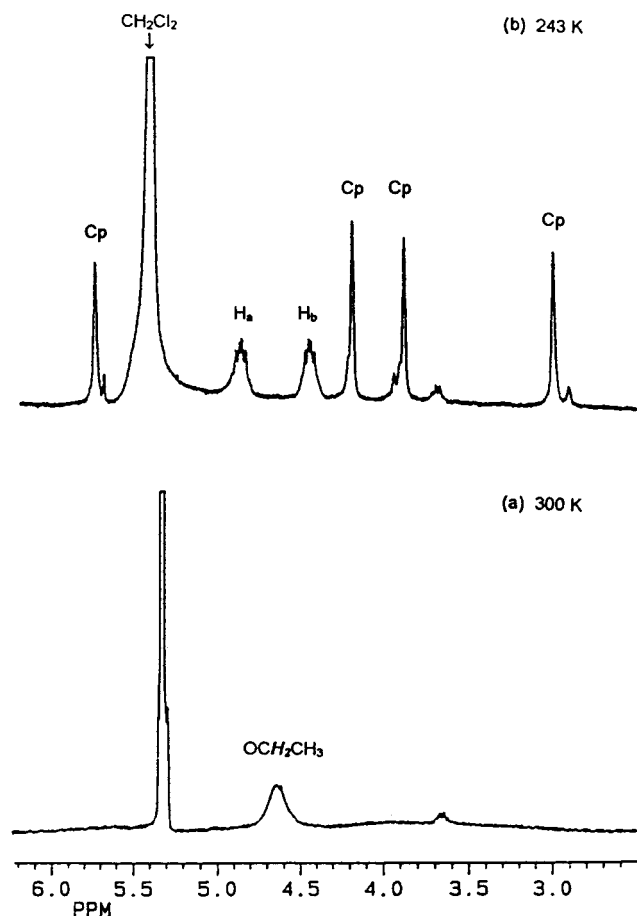


Figure 4. ^1H NMR spectra of $\text{Re}_2(\mu\text{-OEt})_2(\mu\text{-dppf})(\text{CO})_6$ (**3**) at (a) 300 K and (b) 243 K.

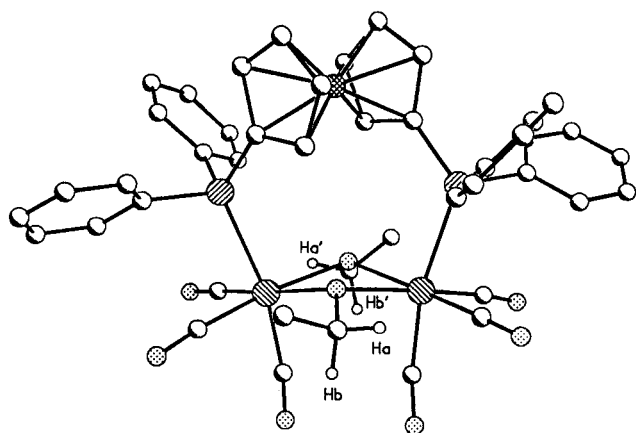


Figure 5. The conformer of $\text{Re}_2(\mu\text{-OEt})_2(\mu\text{-dppf})(\text{CO})_6$ (**3**) with *exo* methyl groups.

attributed to ring current effects from the phenyl groups of the dppf ligand.⁹ Thus, the variable-temperature NMR behavior of the Cp protons can be attributed solely to the freezing-out of the twisting motion of the bridging dppf ligand at lower temperatures, similar to that observed in complex **2**.⁹ The triplet signal due to the terminal methyl groups shows no noticeable change as the temperature is lowered.

Assuming that the crystal structure of complex **3** (with both the methyl groups in *exo* positions (Figure 5)) corresponds closely with that of one of the interconverting conformers of the complex in solution, the two methylene quartets observed at 243 K can be assigned

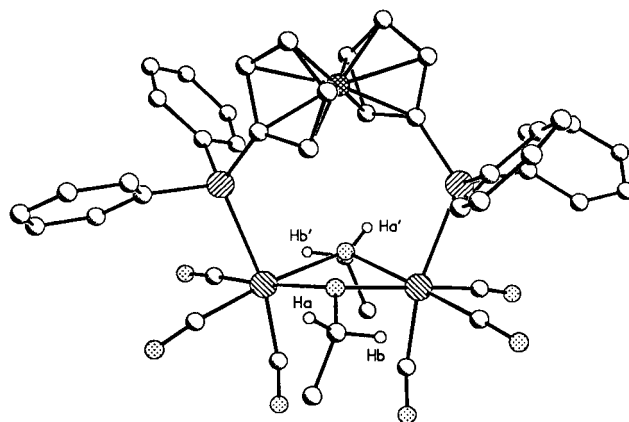
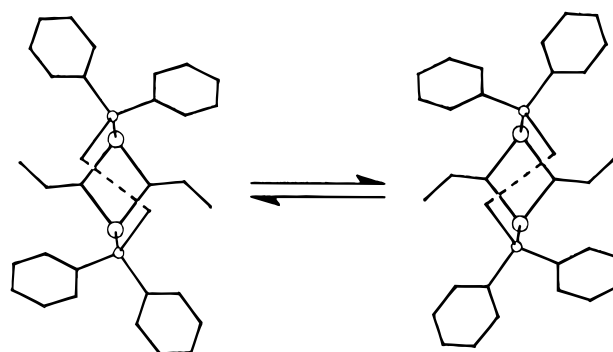


Figure 6. The conformer of $\text{Re}_2(\mu\text{-OEt})_2(\mu\text{-dppf})(\text{CO})_6$ (**3**) with *endo* methyl groups.

Scheme 2



to H_a/H_a' and H_b/H_b' , respectively. The ethyl protons at 243 K can, therefore, be described as an ABX_3 spin system, assuming that the methyl group can still rotate freely at this temperature. This is consistent with the second-order features observed in the methylene proton signals: the lines in the quartets do not have the 1:3:3:1 intensity ratio, and additional lines which appear as shoulders are apparently present.¹¹ The H_a/H_a' and H_b/H_b' positions are exchanged when the dppf bridge twists into the enantiomeric conformation (see Scheme 2), with the concomitant turning of the two ethyl groups toward the phenyl rings (C(11)–C(16) and C(11a)–C(16a), respectively). Since the two exchanging positions for each of the methyl groups are equivalent, the methyl resonance is unaffected by temperature variations. Similar arguments may be put forward for the slow exchange of conformers with only *endo* methyl groups (Figure 6).

Both the *exo* and *endo* conformers of complex **3** can, in principle, co-exist in solution, since the conformers coexist in the ratio of 60:40 in the crystal structure of the complex. Curiously, however, the ^1H NMR spectrum of **3** at 243 K indicates the presence of only one major conformer (since *each* conformer is expected to give rise to two methylene proton signals and four Cp proton signals). Interconversion of the *exo* and *endo* conformers is unlikely in solution at room temperature

(11) The methylene proton signals at 243 K were simulated using the program DSYMPC (see: Hägele, G.; Spiske, R.; Höffken, H. W.; Lenzen, T.; Weber, U.; Goudetsidis, S. *Phosphorus Sulfur* **1993**, *77*, 262) on a Pentium PC. Good agreement with the observed spectrum was obtained with the following parameters: $^2J(\text{H}_a\text{H}_b) = 11.0$ Hz, $^3J(\text{H}_a\text{H}_3\text{C}) = ^3J(\text{H}_b\text{H}_3\text{C}) = 6.5$ Hz, line width = 5.0 Hz.

and below, since rotation of the methyl groups from the *exo* to the *endo* positions is severely hindered by the equatorial CO groups (C(2)–O(2) and C(2a)–O(2a)). This was established by calculating the theoretical position of C(20) when the methyl group is being rotated past the carbonyl group C(2a)–O(2a), *i.e.*, when the torsional angle C(20)–C(10)⋯Re(1a)–C(2a) is 0.0° (C(10)–C(20) bond length set at 1.540 Å and $\angle\text{O}(10)\text{--C}(10)\text{--C}(20)$ set at 114.0° , *cf.* the measured $\angle\text{O}(10)\text{--C}(10)\text{--C}(20)$ of 113.9°). At this position (fractional coordinates 0.82791, 0.11117, 0.53613), the C(20)⋯C(2a) distance is 2.69 Å, which is much shorter than the sum of the van der Waals radii of two carbon atoms¹² (3.70 Å). Although some of the trace “impurity” peaks in the spectrum could possibly be assigned to the minor conformer, this assignment cannot be made with certainty since the minor component that gave rise to these peaks has so far eluded isolation.

Acidolysis of $[\text{Re}_2(\mu\text{-OME})_3(\text{CO})_6]^-$ in the Presence of Monodentate Ligands. The successful synthesis of **1–4** by the controlled acidolysis route prompted us to attempt the analogous synthesis of the complexes $[\text{Re}_2(\mu\text{-OME})_2(\text{CO})_6(\text{PPh}_3)_2]$ and $[\text{Re}_2(\mu\text{-OME})_2(\text{CO})_8]$ by using PPh_3 and CO in place of dppf. An earlier attempt to synthesize $[\text{Re}_2(\mu\text{-OME})_2(\text{CO})_6(\text{PPh}_3)_2]$ by applying the original synthetic strategy for **2**, *i.e.*, by the oxidative decarbonylation of $\text{Re}_2(\text{CO})_{10}$ by Me_3NO in a mixture of THF and MeOH, followed by addition of PPh_3 , was unsuccessful.^{1c} There has also been no report of the complex $[\text{Re}_2(\mu\text{-OME})_2(\text{CO})_8]$, although the complexes $[\text{Re}_2(\mu\text{-X})_2(\text{CO})_8]$ (X = halides) are well-established.¹³

Acidolysis of $[\text{Re}_2(\mu\text{-OME})_3(\text{CO})_6]^-$ in the Presence of PPh_3 . The reaction proceeded very slowly, with little conversion of starting materials even after 4 h (*cf.* the analogous reaction with dppf, which is virtually complete within 1 h). The main product that was isolated after the reaction had proceeded for 24 h was *fac*- $[\text{Re}(\eta^1\text{-OTs})(\text{CO})_3(\text{PPh}_3)_2]$.

The preferential formation of the mononuclear Re complex can be explained by the large bulk of PPh_3 , which would destabilize the dinuclear $\{\text{Re}_2(\mu\text{-OME})_2(\text{PPh}_3)_2\}$ moiety. Cleavage of the dimer followed by PPh_3 scrambling and attack of TsOH would give the observed product *fac*- $[\text{Re}(\eta^1\text{-OTs})(\text{CO})_3(\text{PPh}_3)_2]$. It is noteworthy that the complex $[\text{Re}_2(\mu\text{-OH})_2(\text{CO})_6(\text{py})_2]$ (py = pyridine) has been synthesized in good yield by heating η^5 -indenylrhenium tricarbonyl in wet pyridine at 50°C .¹⁴ In the latter case, the low steric demand of the pyridine ligands allows the $\{\text{Re}_2(\mu\text{-OH})_2\}$ core to remain intact without a third bridging ligand.

Acidolysis of $[\text{Re}_2(\mu\text{-OME})_3(\text{CO})_6]^-$ in the Presence of CO. Reaction of $[\text{Re}_2(\mu\text{-OME})_3(\text{CO})_6]^-$ with TsOH in the presence of CO gas (1 atm) unexpectedly affords the trinuclear complex anion $[\text{Re}_3(\mu\text{-OME})_3(\mu_3\text{-OME})(\text{CO})_9]^-$ (**6**) instead of $[\text{Re}_2(\mu\text{-OME})_2(\text{CO})_8]$. An increase of the CO pressure to 2 atm led to a mixture of numerous trace products which are presently unidentified. The formation of **6** suggests that only one

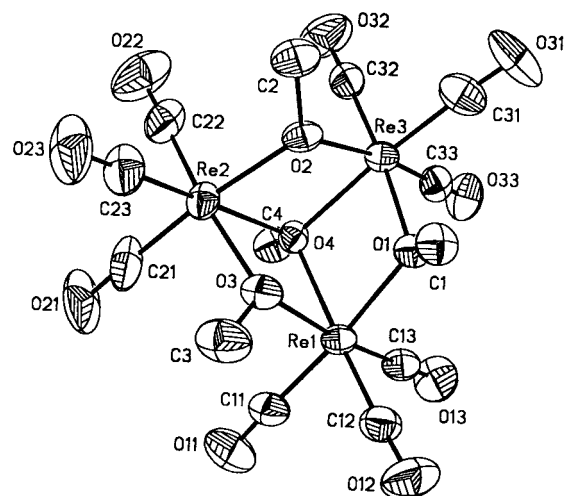
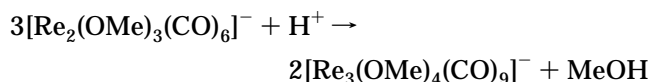


Figure 7. Crystal structure of $[\text{Re}_3(\mu\text{-OME})_3(\mu_3\text{-OME})(\text{CO})_9]^-$ (**6**; 50% probability ellipsoids).

methoxy group is cleaved for every three molecules of $[\text{Re}_2(\mu\text{-OME})_3(\text{CO})_6]^-$ and that the latter complex is not carbonylated in the reaction:



The presence of CO gas is, however, necessary for the synthesis of complex **6**, since the complex is not formed in detectable quantities when the reaction is carried out under an argon atmosphere. This “catalytic” effect of CO can be explained by the stabilizing effect of CO upon the $[\text{Re}(\text{CO})_3]$ moiety formed by cleavage of a Re–O(Me) bond (whereby the formation of a $[\text{Re}(\text{CO})_4]$ moiety would provide temporary stabilization). Subsequent attack of a basic terminal or μ_2 -methoxy group would eliminate a CO and regenerate the $[\text{Re}(\text{CO})_3]$ fragment.

Complex **6** has also been reported as a product of the carbonylation of ammonium perchlorate in methanol at 240°C under a CO pressure (at room temperature) of *ca.* 50 bar.^{6b} The IR and ^1H NMR spectroscopic data for **6** prepared by our method are, however, different from those reported.¹⁵ This prompted us to determine the crystal structure of complex **6**.

Crystal Structure of $[\text{NET}_4][\text{Re}_3(\mu\text{-OME})_3(\mu_3\text{-OME})(\text{CO})_9]^-$ (6**).** The crystal structure of the anion **6** consists of a Re_3 triangle held together by one face-capping and three edge-bridging methoxy groups, with no Re–Re bonds (Figure 7). Its gross structural features are similar to those observed in the analogous complexes $[\text{Re}_3(\mu\text{-OH})_2(\mu\text{-OME})(\mu_3\text{-OME})(\text{CO})_9]^-$ ^{1a} and $[\text{Re}_3(\mu\text{-OH})_3(\mu_3\text{-OH})(\text{CO})_9]^-$, ^{6a} whose structures can be described in terms of a $\{\text{Re}_4\text{O}_4\}$ cube with a missing Re vertex. However, while there is no significant difference in the bond lengths between Re and μ - or μ_3 -OH in $[\text{Re}_3(\mu\text{-OH})_3(\mu_3\text{-OH})(\text{CO})_9]^-$ (average 2.157(7) and 2.167(6) Å, respectively), the Re–(μ_3 -OME) bond lengths (average 2.202(5) Å) are significantly longer than the Re–(μ -

(12) Emsley, J. *The Elements*; Clarendon Press: Oxford, 1989; p 46.

(13) Boag, N. M.; Kaesz, H. D. In *Comprehensive Organometallic Chemistry*, 1st ed.; Wilkinson, G., Stone, F. G. A., Abel, E. W., Eds.; Pergamon: Oxford, 1982; Vol. 4, p 161.

(14) Zdanovich, V. I.; Lobanova, I. A.; Petrovskii, P. V.; Batsanov, A. S.; Struchkov, Yu. T.; Kolobova, N. E. *Bull. Acad. Sci. USSR, Div. Chem. Sci.* **1987**, 36, 1500.

(15) Herrmann *et al.* reported ν_{CO} bands at 1991 s, 1878 vs, and 1867 vs cm^{-1} (in THF). The ν_{CO} bands we observed generally occur at higher wavenumbers: 2021 w, 2003 s, 1892 vs, 1878 s(sh) cm^{-1} (in THF). In the reported ^1H NMR ($(\text{CD}_3)_2\text{CO}$) data, the signals of the methoxy protons occur at δ 3.70 (s, 3H) and 4.23 (s, 9H), respectively. We observed the corresponding signals at δ 4.52 and 4.24, respectively, in the same solvent.

OMe) bond lengths (average 2.129(5) Å) in **6**. This is probably due to the larger steric hindrance experienced by the μ_3 -OMe group compared to the μ_3 -OH group (apart from the expected weaker interaction of the Re atoms with a μ_3 -OR group, which is less basic than μ_2 -OR groups). The bulkier methoxy groups do not cause any significant expansion of the Re₃ triangle, however, as shown by the close similarity between the range of Re...Re distances in **6** (3.42–3.44 Å) and those observed in [Re₃(μ -OH)₂(μ -OMe)(μ_3 -OMe)(CO)₉]⁻ (3.42–3.44 Å) and [Re₃(μ -OH)₃(μ_3 -OH)(CO)₉]⁻ (3.41–3.44 Å).

Concluding Remarks. Controlled acidolysis of [Re₂(μ -OR)₃(CO)₆]⁻ complexes in the presence of dppf provides a convenient general route to the complexes [Re₂(μ -OR)₂(μ -dppf)(CO)₆] (R = H, Me, Et, Ph). The latter complexes exhibit fluxionality in solution at room temperature, in the form of the twisting of the ferrocenyl moiety of the dppf ligand with respect to the Re...Re axis. This twisting motion is correlated with the restricted rotation of the ethyl groups about the O-CH₂ bonds in the ethoxy complex [Re₂(μ -OEt)₂(μ -dppf)(CO)₆], which provides an interesting example of a situation in which the two exchanging positions of the methylene protons of an ethyl group are nonequivalent while the exchanging positions of the methyl group are equivalent. Controlled acidolysis of [Re₂(μ -OMe)₃(CO)₆]⁻ under 1 atm of CO pressure affords the complex [Re₃(μ -OMe)₃(μ_3 -OMe)(CO)₉]⁻ instead of [Re₂(μ -OMe)₂(CO)₈]. This may be attributed to the strong tendency of OMe groups to function as bridging ligands,¹⁶ the relative lability of CO ligands, and the low steric hindrance of CO and OMe ligands against the aggregation of [Re(OMe)(CO)₃] fragments. Similar reasons may be invoked to explain the fact that [Re(OMe)(CO)₅] has so far eluded isolation.

Experimental Section

All reactions were performed under pure dry argon using standard Schlenk techniques. Solvents used were of reagent grade and were dried by published procedures¹⁷ and freshly distilled under argon before use. The complex [ReBr(CO)₅] was prepared according to reported procedures.¹⁸ All other reagents were of AR grade and were obtained from commercial sources. Precoated silica plates of layer thickness 0.25 mm were obtained from Merck. ¹H and ³¹P{¹H} NMR spectra were recorded at ca. 300 K at field strengths of 300.0 and 121.5 MHz, respectively. ¹H and ³¹P chemical shifts are quoted in ppm downfield of tetramethylsilane and external 80% H₃PO₄, respectively. Elemental analyses were performed by the Microanalytical Laboratory, Department of Chemistry, National University of Singapore.

[NEt₄][Re₂(μ -OH)₃(CO)₆]. Aqueous NaOH (0.2 M, 5 mL) was added to a solution of ReBr(CO)₅ (0.082 g, 0.2 mmol) in 20 mL of THF and 5 mL of H₂O. The resultant mixture was stirred under vacuum at room temperature for 1 h and then under argon for 20 h. The solvent was removed under reduced pressure, and the solid residue obtained was redissolved in 5 mL of H₂O. The solution was filtered and treated with a solution of [NEt₄]Cl (0.33 g, 2.0 mmol) in H₂O (5 mL). The resultant solution was kept at 10 °C for 1 week. The colorless

cubic crystals of [NEt₄][Re₂(μ -OH)₃(CO)₆] formed were isolated by filtration and dried under vacuum. Yield 0.052 g (72%). Anal. Calcd for C₁₄H₂₃NO₉Re₂: C, 23.3; H, 3.2; N, 1.9. Found: C, 23.2; H, 3.2; N, 2.0. IR (cm⁻¹): CH₂Cl₂ ν (C-O) 2007 (vw), 1996 (m), 1878 (vs); KBr ν (O-H) 3639 (m).

The recovery of the anion was increased to 90% when [NBu₄]⁺Br⁻ was used as the precipitant, in which case the salt was obtained as white microcrystals after 1 day at 10 °C.

[NEt₄][Re₂(μ -OR)₃(CO)₆] (R = Me, Et). In a typical synthesis, a 1 M solution of NaOR in ROH was prepared by the reaction of sodium (0.23 g, 10 mmol) with 10 mL of the alcohol. A 0.6 mL amount of the 1 M NaOR/ROH solution was added to a solution of ReBr(CO)₅ (0.082 g, 0.2 mmol) in 20 mL of THF and 10 mL of ROH. The resultant mixture was stirred under vacuum at room temperature for 1 h and then under argon for 20 h. The solvent was removed under reduced pressure, and the solid residue obtained was redissolved in 5 mL of ROH. The solution was filtered and treated with a solution of [NEt₄]Cl (0.33 g, 2.0 mmol) in H₂O (5 mL). The resultant solution was kept at -10 °C for 1–2 days. The precipitate of [NEt₄][Re₂(μ -OR)₃(CO)₆] obtained was isolated by filtration and dried under vacuum.

[NEt₄][Re₂(μ -OMe)₃(CO)₆]. Colorless needle-shaped crystals. Yield 0.065 g (85%). Anal. Calcd for C₁₇H₂₉NO₉Re₂: C, 26.7; H, 3.8; N, 1.8. Found: C, 26.1; H, 3.8; N, 1.9.¹⁹ IR (cm⁻¹): CH₂Cl₂ ν (C-O) 1993 (s), 1876 (vs). ¹H NMR ((CD₃)₂CO): δ 4.20 (s, 9H, μ -OMe).

[NEt₄][Re₂(μ -OEt)₃(CO)₆]. White powder. Yield 0.055 g (68%). Anal. Calcd for C₂₀H₃₅NO₉Re₂: C, 29.8; H, 4.4; N, 1.7. Found: C, 29.8; H, 4.4; N, 1.7. IR (cm⁻¹): CH₂Cl₂ ν (C-O) 1990 (s), 1872 (vs). ¹H NMR (CDCl₃): δ 4.24 (q, 6H, μ -OCH₂CH₃), 1.28 (t, 9H, μ -OCH₂CH₃).

[NEt₄][Re₂(μ -OH)(μ -OPh)₂(CO)₆] (5). A 1 M solution of NaOPh in THF was prepared by the reaction of sodium (0.115 g, 5 mmol) with phenol (0.565 g, 6 mmol, dried under vacuum at room temperature and weighed in a glovebox) in freshly-distilled THF. A 0.6 mL amount of this solution and 0.1 mL of wet THF ([H₂O] \approx 1 M, prepared by the addition of 0.18 mL (ca. 10 mmol) of water to 10 mL of dried THF) were added to a solution of ReBr(CO)₅ (0.082 g, 0.2 mmol) in 20 mL of THF. The resultant mixture was stirred under vacuum at room temperature for 1 h and then under argon for 20 h. The solvent was removed under reduced pressure, and the solid residue obtained was redissolved in 10 mL of H₂O. The solution was filtered and treated with a solution of [NEt₄]Cl (0.33 g, 2.0 mmol) in H₂O (5 mL). The resultant solution was kept at 10 °C for 1–2 days, during which a white powdery precipitate of [NEt₄][Re₂(μ -OH)(μ -OPh)₂(CO)₆] (**5**) was formed. The solid was separated by filtration, dried under vacuum, and recrystallized by layering a solution of the compound in CH₂-Cl₂ with hexane. Colorless prismatic crystals of [NEt₄][Re₂(μ -OH)(μ -OPh)₂(CO)₆] were obtained. Yield 0.065 g (74%). Anal. Calcd for C₂₆H₃₁NO₉Re₂: C, 35.7; H, 3.6; N, 1.6. Found: C, 34.6; H, 3.6; N, 1.6.¹⁹ IR (cm⁻¹): CH₂Cl₂ ν (C-O) 2003 (s), 1886 (vs); KBr ν (O-H) 3648 (m). ¹H NMR: CD₂Cl₂ δ 7.26–7.16 (m, 8H, Ph), 6.76 (tt, 2H, Ph), 2.92 (q, 8H, NCH₂-CH₃), 1.14 (tt, 12H, NCH₂CH₃).

[Re₂(μ -OH)₂(μ -dppf)(CO)₆] (1). A solution of TsOH·H₂O (recrystallized from hot water) (0.038 g, 0.20 mmol) in 10 mL of THF was transferred into a stirred solution of [NEt₄][Re₂(μ -OH)₃(CO)₆] (0.145 g, 0.20 mmol) and dppf (0.112 g, 0.20 mmol) in 20 mL of THF. The resultant mixture was stirred under argon for 3 h. The solution was then concentrated to 10 mL and filtered. Water (20 mL) was added to the filtered chrome-yellow solution, and the mixture was kept at 10 °C for 24 h. The yellow precipitate formed was filtered and

(16) Cotton, F. A.; Wilkinson, G. *Advanced Inorganic Chemistry*, 5th ed.; Wiley-Interscience: Singapore, 1988; p 472.

(17) Gordon, A. J.; Ford, R. A. *The Chemist's Companion: A Handbook of Practical Data, Techniques and References*; Wiley-Interscience: New York, 1972.

(18) (a) Albano, V. G.; Bellon, P. L.; Sansoni, M. *J. Chem. Soc. A* **1971**, 2420. (b) Angelici, R. J.; Kruse, A. E. *J. Organomet. Chem.* **1970**, *22*, 461.

(19) The carbon analysis was consistently lower than the calculated value, despite excellent agreement for the H and N analyses, possibly due to the formation of a small amount of refractory rhenium carbide during combustion analysis.

Table 2. Crystallographic Data for Compounds 1, 3, 5, and 6

	1	3	5	6
chemical formula	$\text{C}_{40}\text{H}_{30}\text{FeO}_8\text{P}_2\text{Re}_2(\text{C}_3\text{H}_6\text{O})_{2.5}$	$\text{C}_{47}\text{H}_{38}\text{FeO}_8\text{P}_2\text{Re}_2$	$\text{C}_{26}\text{H}_{31}\text{NO}_9\text{Re}_2$	$\text{C}_{21}\text{H}_{32}\text{NO}_{13}\text{Re}_3$
space group	$P1$	$C2/c$	$P2_1/n$	$P1$
unit cell dimens				
a (Å)	12.037(3)	20.664(3)	13.479(3)	10.195(5)
b (Å)	12.781(3)	15.369(2)	14.601(4)	11.436(5)
c (Å)	16.877(4)	17.129(2)	14.888(3)	13.493(5)
α (deg)	109.37(2)	90	90	96.56(3)
β (deg)	99.17(2)	122.231(9)	102.850(10)	99.54(3)
γ (deg)	97.31(2)	90	90	96.62(3)
V (Å ³)	2372.5(10)	4601.8(10)	2856.7(12)	1526.8(11)
Z	2	4	4	2
cryst size (mm)	$0.25 \times 0.24 \times 0.44$	$0.13 \times 0.20 \times 0.40$	$0.08 \times 0.15 \times 0.30$	$0.07 \times 0.20 \times 0.40$
μ (mm ⁻¹)	5.59	5.679	8.518	11.921
min, max transmission	0.677, 0.999	0.5976, 0.8455	0.4894, 0.9487	0.3452, 0.9798
diffractometer	Nonius	Siemens P4	Siemens P4	Siemens P4
max 2θ (deg)	49.9	47.0	45.1	50.0
hkl range	-14 to 14, 0 to 15, -20 to 18	-1 to 23, to 1 to 17, to 19 to 16	-1 to 14, to 1 to 15, to 16 to 15	-1 to 12, to 13 to 13, to 16 to 15
no. of reflns measd	8777	4066	4667	6343
no. of unique reflns (R_{int})	8341 (0.012)	3412 (0.038)	3707 (0.039)	5357 (0.017)
R_1, b w R^c ($I > 2 \sigma(I)$)	0.032, 0.035 (R_w) ^d	0.0448, 0.1225	0.0438, 0.1017	0.0296, 0.0718

^a Details in common: temperature of 296 ± 2 K, graphite-monochromated Mo K α radiation, θ - 2θ scan mode, empirical ψ absorption corrections. ^b $R_1 = \sum ||F_o| - |F_c|| / \sum |F_o|$. ^c $wR = [\sum w(F_o^2 - F_c^2)^2 / \sum w(F_o^2)]^{1/2}$. ^d $R_w = [\sum w(|F_o| - |F_c|)^2 / \sum w|F_o|^2]^{1/2}$.

recrystallized from acetone (slow evaporation at 10 °C). Yellow prismatic crystals of $\text{Re}_2(\mu\text{-OH})_2(\mu\text{-dppf})(\text{CO})_6$ (**1**) were formed. The crystals became opaque soon after leaving the mother liquor. Yield 0.198 g (88%). Anal. Calcd for $\text{C}_{40}\text{H}_{30}\text{FeO}_8\text{P}_2\text{Re}_2$: C, 42.6; H, 2.7; P, 5.5. Found: C, 42.7; H, 2.7; P, 5.5. IR (cm⁻¹): CH_2Cl_2 $\nu(\text{C}-\text{O})$ 2026 (s), 2009 (m), 1920 (m), 1898 (vs), 1888 (s, sh); KBr $\nu(\text{O}-\text{H})$ 3600 (m). ¹H NMR: CD_2Cl_2 δ 7.43 (br s, 20H, Ph), 5.5–4.5 (vbr s, 4H, Cp), 3.8–3.4 (vbr s, 4H, Cp), -0.38 (t, ³J(HP) = 1.3 Hz, 2H, $\mu\text{-OH}$) [cf. $\delta(\text{OH})$ -0.35, ³J(HP) = 4.0 Hz for $\text{Re}_2(\mu\text{-OH})_2(\mu\text{-dppm})(\text{CO})_6$].³ ³¹P{¹H} NMR (CD_2Cl_2): δ 3.0.

[Re₂(μ -OMe)₂(μ -dppf)(CO)₆] (2). A solution of TsOH·H₂O (0.038 g, 0.20 mmol) in 10 mL of CHCl₃ and 10 mL of MeOH was transferred into a stirred solution of [NET₄][Re₂(μ -OMe)₃(CO)₆] (0.152 g, 0.20 mmol) and dppf (0.112 g, 0.20 mmol) in 10 mL of CHCl₃. The resultant mixture was stirred under argon for 1 h. The solvent was then removed under reduced pressure. The residue obtained was redissolved in a minimum amount of CHCl₃ and chromatographed on silica TLC plates (CH₂Cl₂/hexane 2:3). Complex **2** was isolated from the main band (R_f 0.50) and was recrystallized from a CH₂Cl₂-MeOH mixture and identified by IR and ¹H and ³¹P NMR spectroscopy.^{1b} Yield 0.164 g (71%).

[Re₂(μ -OEt)₂(μ -dppf)(CO)₆] (3). The procedure was similar to that described for complex **2** except that [NET₄][Re₂(μ -OEt)₃(CO)₆] (0.161 g, 0.20 mmol) and EtOH were used instead of [NET₄][Re₂(μ -OMe)₃(CO)₆] and MeOH. Removal of solvent followed by TLC (CH₂Cl₂/hexane 2:3) yielded complex **3** (R_f 0.47), which was then recrystallized from CH₂Cl₂-EtOH solution at -10 °C. Yield 0.028 g (12%, chrome-yellow microcrystals). Anal. Calcd for $\text{C}_{44}\text{H}_{38}\text{FeO}_8\text{P}_2\text{Re}_2(\text{CH}_2\text{Cl}_2)_{0.5}$: C, 43.5; H, 3.2; P, 5.0. Found: C, 43.8; H, 3.2; P, 5.2. IR (cm⁻¹): CH_2Cl_2 $\nu(\text{C}-\text{O})$ 2025 (vs), 2008 (s), 1920 (s), 1898 (vs), 1890 (s, sh). ¹H NMR: CD_2Cl_2 δ 7.46 (br s, 20H, Ph), 4.65 (br s, 4H, CH₂), 1.45 (t, ³J(HH) = 6.2 Hz, 6H, CH₃). ³¹P{¹H} NMR (CD_2Cl_2): δ 3.6.

[Re₂(μ -OPh)₂(μ -dppf)(CO)₆] (4). A solution of TsOH·H₂O (0.038 g, 0.20 mmol) in 20 mL of CHCl₃ was transferred into a stirred suspension of [NET₄][Re₂(μ -OH)(μ -OPh)₂(CO)₆] (0.175 g, 0.20 mmol) and dppf (0.112 g, 0.20 mmol) in 20 mL of CHCl₃. The resultant mixture was stirred under argon for 1 h. The solvent was then removed under reduced pressure. The residue obtained was redissolved in a minimum amount of CHCl₃ and chromatographed on silica TLC plates (CH₂Cl₂/hexane 2:3). Complex **4** was isolated from the main band (R_f 0.56) and recrystallized from CH₂Cl₂-hexane solution at -10

°C. Yield 0.095 g (36%, yellow powder). Anal. Calcd for $\text{C}_{52}\text{H}_{38}\text{FeP}_2\text{O}_8\text{Re}_2 \cdot 0.5\text{CH}_2\text{Cl}_2$: C, 47.6; H, 3.0; P, 4.7. Found: C, 47.3; H, 3.1; P, 4.8. IR (cm⁻¹): CH_2Cl_2 $\nu(\text{C}-\text{O})$ 2024 (s), 2008 (m), 1916 (m, sh), 1899 (vs), 1887 (s, sh). ¹H NMR: CD_2Cl_2 δ 7.8–7.1 (vbr m, 30H, Ph), 4.8–4.6 (br s, 4H, Cp), 3.8–3.7 (vbr s, 4H, Cp); (CD_3)₂CO δ 7.8–7.1 (vbr m, 30H, Ph), 4.7–4.5 (br s, 4H, Cp), 3.8–3.5 (vbr s, 4H, Cp). ³¹P{¹H} NMR: CD_2Cl_2 δ 3.6; (CD_3)₂CO δ 2.6.

Acidolysis of [Re₂(μ -OMe)₃(CO)₆] in the presence of PPh₃. The procedure was similar to that described for complex **2**, except that PPh₃ (0.106 g, 0.40 mmol) was used instead of dppf (0.112 g, 0.20 mmol) and that the reaction was allowed to proceed for 24 h. Removal of solvent followed by TLC (CH₂Cl₂/hexane 2:3) revealed the presence of numerous products which were formed in minute quantities. The complex [*fac*-Re(η^1 -OTs)(CO)₃(PPh₃)₂] was isolated from the main band (R_f 0.08) and recrystallized by layering a solution of the complex in CH₂Cl₂ with hexane. Yield 0.020 g (12%, colorless prismatic crystals). Anal. Calcd for $\text{C}_{46}\text{H}_{37}\text{O}_6\text{P}_2\text{ReS}$: C, 57.2; H, 3.8; S, 3.3; P, 6.4. Found: C, 57.8; H, 4.0; S, 2.8; P, 6.7. IR (cm⁻¹): CH_2Cl_2 $\nu(\text{C}-\text{O})$ 2041 (s), 1960 (m), 1908 (m). ¹H NMR: CD_2Cl_2 δ 7.4–7.0 (m, 34H, Ph), 2.35 (s, 3H, CH₃). ³¹P{¹H} NMR (CD_2Cl_2): δ 9.2.

Acidolysis of [Re₂(μ -OMe)₃(CO)₆] in the presence of CO. Carbon monoxide was bubbled through a stirred solution of [NET₄][Re₂(μ -OMe)₃(CO)₆] (0.152 g, 0.20 mmol) in 20 mL of CHCl₃. About 10 min later, a solution of TsOH·H₂O (0.038 g, 0.20 mmol) in 10 mL of CHCl₃ and 10 mL of MeOH was transferred into the above CO-saturated solution. The mixture was stirred at room temperature for 24 h, with CO being bubbled through at a slow rate. The solvent was removed under reduced pressure, and the residue obtained was redissolved in a minimum amount of CHCl₃ and chromatographed on silica TLC plates (CHCl₃). The main band (R_f 0.08) was extracted with CH₂Cl₂, and the concentrated extract was layered with hexane. Colorless prismatic crystals of [NET₄]-[Re₃(μ_3 -OMe)(μ -OMe)₃(CO)₉] were obtained (0.018 g, 13%). Anal. Calcd for $\text{C}_{21}\text{H}_{32}\text{NO}_{13}\text{Re}_3$: C, 23.7; H, 3.0; N, 1.3. Found: C, 23.9; H, 3.1; N, 1.5. IR (cm⁻¹): CH_2Cl_2 $\nu(\text{C}-\text{O})$ 2023 (w), 2004 (s), 1893 (vs), 1879 (s, sh); THF 2021 (w), 2003 (s), 1892 (vs), 1878 (s, sh). ¹H NMR: (CD_3)₂CO δ 4.52 (s, 3H, μ_3 -OMe), 4.24 (s, 9H, μ -OMe); CD_2Cl_2 δ 4.51 (s, 3H, μ_3 -OMe), 4.30 (s, 9H, μ -OMe).

X-ray Crystallography. The crystallographic data for compounds **1**, **3**, **5**, and **6** are summarized in Table 2, and selected bond lengths and angles are given in Tables 3–6.

Table 3. Bond Lengths (Å) and Angles (deg) for 1

Re(1)–P(1)	2.5147(23)	Re(2)–P(2)	2.5307(21)
Re(1)–C(1)	1.899(9)	Re(2)–C(4)	1.895(9)
Re(1)–C(2)	1.921(9)	Re(2)–C(5)	1.933(9)
Re(1)–C(3)	1.903(9)	Re(2)–C(6)	1.890(9)
Re(1)–O(7)	2.171(5)	Re(2)–O(7)	2.153(5)
Re(1)–O(8)	2.170(5)	Re(2)–O(8)	2.178(5)
C(1)–Re(1)–P(1)	83.4(3)	C(6)–Re(2)–P(2)	88.3(3)
C(2)–Re(1)–P(1)	167.4(3)	C(4)–Re(2)–O(8)	170.7(3)
C(3)–Re(1)–P(1)	88.3(3)	C(5)–Re(2)–O(8)	94.6(3)
C(1)–Re(1)–O(7)	172.3(3)	C(6)–Re(2)–O(8)	101.1(3)
C(2)–Re(1)–O(7)	94.6(3)	C(4)–Re(2)–C(5)	85.6(4)
C(3)–Re(1)–O(7)	97.2(3)	C(4)–Re(2)–C(6)	88.1(4)
C(1)–Re(1)–C(2)	86.1(4)	C(5)–Re(2)–C(6)	83.4(4)
C(1)–Re(1)–C(3)	90.5(4)	O(7)–Re(2)–O(8)	70.81(18)
C(2)–Re(1)–C(3)	84.7(4)	Re(1)–O(7)–Re(2)	104.45(20)
O(7)–Re(1)–O(8)	70.61(18)	Re(1)–O(8)–Re(2)	103.64(20)
C(4)–Re(2)–P(2)	85.53(25)	C(51)–P(1)–Re(1)	120.6(3)
C(5)–Re(2)–P(2)	168.1(3)	C(56)–P(2)–Re(2)	123.0(3)

Table 4. Bond Lengths (Å) and Angles (deg) for 3^a

Re(1)–P(1)	2.543(3)	Re(1)–O(10a)	2.189(8)
Re(1)–C(1)	1.930(14)	O(10)–C(10)	1.421(9)
Re(1)–C(2)	1.910(14)	C(10)–C(20)	1.503(10)
Re(1)–C(3)	1.88(2)	C(10)–C(20')	1.514(10)
Re(1)–O(10)	2.190(7)		
C(1)–Re(1)–P(1)	168.0(4)	C(2)–Re(1)–C(3)	86.6(6)
C(2)–Re(1)–P(1)	87.4(4)	O(10a)–Re(1)–O(10)	72.8(3)
C(3)–Re(1)–P(1)	85.9(4)	C(10)–O(10)–Re(1a)	123.0(7)
C(1)–Re(1)–O(10)	92.3(4)	C(10)–O(10)–Re(1)	113.7(8)
C(2)–Re(1)–O(10)	172.3(4)	Re(1a)–O(10)–Re(1)	103.2(3)
C(3)–Re(1)–O(10)	99.8(5)	O(10)–C(10)–C(20)	113.9(10)
C(1)–Re(1)–C(2)	84.0(5)	O(10)–C(10)–C(20')	113.2(10)
C(1)–Re(1)–C(3)	85.3(6)	C(31)–P(1)–Re(1)	123.7(4)

^a Symmetry transformations used to generate equivalent atoms: $-x + 2, y, -z + 3/2$.

Table 5. Bond Lengths (Å) and Angles (deg) for 5

Re(1)–Re(2)	3.1519(9)	Re(2)–O(10)	2.163(9)
Re(1)–O(10)	2.162(8)	Re(2)–O(20)	2.151(8)
Re(1)–O(20)	2.149(8)	Re(2)–O(30)	2.118(9)
Re(1)–O(30)	2.138(9)	Re(2)–C(4)	1.88(2)
Re(1)–C(1)	1.89(2)	Re(2)–C(5)	1.88(2)
Re(1)–C(2)	1.89(2)	Re(2)–C(6)	1.91(2)
Re(1)–C(3)	1.88(2)		
Re(1)–O(10)–Re(2)	93.6(3)	O(10)–Re(1)–O(30)	72.8(3)
Re(1)–O(20)–Re(2)	94.3(3)	O(20)–Re(1)–O(30)	71.5(4)
Re(1)–O(30)–Re(2)	95.5(4)	O(10)–Re(2)–O(20)	71.4(3)
C(1)–Re(1)–C(2)	86.0(6)	O(10)–Re(2)–O(30)	73.1(4)
C(1)–Re(1)–C(3)	88.7(6)	O(20)–Re(2)–O(30)	71.9(3)
C(2)–Re(1)–C(3)	88.0(7)	C(11)–O(10)–Re(1)	136.0(8)
C(4)–Re(2)–C(5)	86.0(7)	C(11)–O(10)–Re(2)	130.1(8)
C(4)–Re(2)–C(6)	85.1(7)	C(21)–O(20)–Re(1)	133.1(7)
C(5)–Re(2)–C(6)	88.0(6)	C(21)–O(20)–Re(2)	132.6(7)
O(10)–Re(1)–O(20)	71.5(3)		

Computations for **1** were carried out on a Microvax 3600 computer with the NRCVAX system,²⁰ while computations for **3**, **5**, and **6** were carried out on a Pentium PC using the SHELXTL PLUS software package.²¹

[Re₂(μ-OH)₂(μ-dppf)(CO)₆] **(1). Single orange crystals of **1** were grown by the slow evaporation of a solution of the complex in acetone at 10 °C. As crystals of **1** desolvate readily on leaving the mother liquor, the crystal used for data collection was sealed in a lithium glass capillary. The number of data used for structure solution and refinement was 5850 ($I > 2.0\sigma(I)$). The structure was solved by direct methods (MULTAN²²). Refinement (on F) was carried out by the full-matrix least-squares method with all non-hydrogen atoms**

(20) Gabe, E. J.; Le Page, Y.; Charland, J.-P.; Lee, F. L.; White, P. S. *J. Appl. Crystallogr.* **1989**, *22*, 384.

(21) Sheldrick, G. M. *SHELXTL PC*, Version 5.03; Siemens Analytical X-ray Instruments, Inc.: Madison, WI, 1994.

Table 6. Bond Lengths (Å) and Angles (deg) for 6

Re(1)–C(11)	1.915(8)	Re(2)–O(4)	2.183(5)
Re(1)–C(12)	1.891(8)	Re(3)–C(31)	1.896(9)
Re(1)–C(13)	1.910(8)	Re(3)–C(32)	1.902(8)
Re(1)–O(1)	2.134(5)	Re(3)–C(33)	1.906(8)
Re(1)–O(3)	2.135(5)	Re(3)–O(1)	2.124(4)
Re(1)–O(4)	2.213(4)	Re(3)–O(2)	2.129(5)
Re(2)–C(21)	1.915(9)	Re(3)–O(4)	2.210(5)
Re(2)–C(22)	1.914(9)	O(1)–C(1)	1.412(8)
Re(2)–C(23)	1.893(8)	O(2)–C(2)	1.425(8)
Re(2)–O(2)	2.132(5)	O(3)–C(3)	1.406(9)
Re(2)–O(3)	2.122(5)	O(4)–C(4)	1.466(8)
Re(1)–O(1)–Re(3)	106.9(2)	O(1)–Re(3)–O(2)	81.2(2)
Re(2)–O(2)–Re(3)	106.6(2)	O(1)–Re(3)–O(4)	75.1(2)
Re(1)–O(3)–Re(2)	107.8(2)	O(2)–Re(3)–O(4)	74.3(2)
Re(1)–O(4)–Re(2)	103.0(2)	C(1)–O(1)–Re(1)	119.9(4)
Re(1)–O(4)–Re(3)	101.3(2)	C(1)–O(1)–Re(3)	121.4(4)
Re(2)–O(4)–Re(3)	102.1(2)	C(2)–O(2)–Re(2)	120.8(5)
O(1)–Re(1)–O(3)	82.2(2)	C(2)–O(2)–Re(3)	119.3(5)
O(1)–Re(1)–O(4)	74.8(2)	C(3)–O(3)–Re(1)	121.1(5)
O(3)–Re(1)–O(4)	73.5(2)	C(3)–O(3)–Re(2)	122.1(5)
O(2)–Re(2)–O(3)	81.4(2)	C(4)–O(4)–Re(1)	115.5(4)
O(2)–Re(2)–O(4)	74.9(2)	C(4)–O(4)–Re(2)	116.5(4)
O(3)–Re(2)–O(4)	74.3(2)	C(4)–O(4)–Re(3)	116.2(4)

(except those of the acetone solvate molecules) being allowed anisotropic motion. All hydrogen atoms were held fixed in the final cycles of least-squares refinement. During the structure refinement, 2.5 acetone solvate molecules were found, the third one being disordered—three independent non-H sites connected with three inversion-related sites, making a total of six for four non-H atoms of acetone. A combined scattering curve Oa was constructed as ($1/6\text{O} + 5/6\text{C}$), and a combined scattering curve Ob was constructed as ($1/3\text{O} + 2/3\text{C}$). The contributions of the third acetone solvate molecule to the structure factors were the summation of two Oa positions, each with half occupancy, and one Ob, with full occupancy. The last least-squares cycle was calculated with 523 parameters and 5850 reflections. The weighting function used was $w^{-1} = \sigma^2(F_o) + 0.000100F_o^2$, and the secondary extinction coefficient²³ was 0.12(5). The maximum shift/ σ ratio was 0.026. In the last difference map, the deepest hole was $-0.700 \text{ e}/\text{Å}^3$ and the highest peak was $0.960 \text{ e}/\text{Å}^3$.

[Re₂(μ-OEt)₂(μ-dppf)(CO)₆] **(3). Single chrome-yellow crystals of **3** were grown by the slow evaporation of a solution of the complex in a CH_2Cl_2 –hexane mixture at 10 °C. The number of data used for structure solution and refinement was 2563 ($I > 2.0\sigma(I)$). The structure was solved by the heavy-atom method. All non-hydrogen atoms (except those of the disordered solvate molecule and the disordered methyl carbon atoms) were refined anisotropically by the full-matrix least-squares method (on F^2). Hydrogen atoms were introduced in calculated positions and refined isotropically (riding model) in the final cycles of least-squares refinement. The disordered ethyl group was refined with two positions for the methyl carbon (C(20) and C(20')), having occupancies of 60% and 40%, respectively, and the distance constraints $\text{O}(10)–\text{C}(10) = 1.43 \pm 0.01$, $\text{C}(10)–\text{C}(20)/\text{C}(20') = 1.54 \pm 0.01$, and $\text{O}(10)–\text{C}(20)/\text{C}(20') = 2.43 \pm 0.01$. The relatively large thermal parameter ($U(\text{eq}) 0.108(7) \text{ Å}^2$) and elongated shape of the thermal ellipsoid of the methylene carbon C(10) suggest that the methylene group is also disordered. An attempt to refine the structure based on a disordered methylene carbon (by splitting the atom along the direction of maximum displacement) did not improve the R values. The severely-disordered solvate molecule is located about a crystallographic inversion center and is**

(22) Main, P.; Fiske, S. E.; Hull, S. L.; Germain, G.; Declercq, J. P.; Woolfson, M. M. *MULTAN, a System of Computer Programs for Crystal Structure Determination from X-ray Diffraction Data*; Universities of York (UK) and Louvain (Belgium), 1980.

(23) The refined parameter is the average path length in a mosaic block in μm , see: Larson, A. C. In *Crystallographic Computing*; Ahmed, F. R., Ed.; Munksgaard: Copenhagen, 1970; p 293.

probably CH_2Cl_2 or *n*-hexane. Yet, as reasonable models of either CH_2Cl_2 or *n*-hexane could not be constructed, C100, C200, and C300 (all half occupancy) per asymmetric unit were refined to account for the scattering in the solvate region. The last least-squares cycle was calculated with 269 parameters and all of the 3412 unique reflections. The weighting function used was $w^{-1} = \sigma^2(F_o^2) + (0.0700P)^2 + 27.0000P$, where $P = (F_o^2 + 2F_c^2)/3$. The maximum shift/ σ ratio was 0.004. In the last difference map, the deepest hole was $-1.009 e/\text{\AA}^3$ and the highest peak was $1.798 e/\text{\AA}^3$ (within 1 \AA from the Re atom).

[NEt₄][Re₂(μ -OH)(μ -OPh)₂(CO)₆] (5). Single colorless crystals of **5** were grown by layering a solution of the compound in CH_2Cl_2 with hexane. The number of data used for structure solution and refinement was 2742 ($I > 2.0\sigma(I)$). The structure was solved by direct methods. All non-hydrogen atoms were refined anisotropically by the full-matrix least-squares method (on F^2). Hydrogen atoms were introduced in calculated positions and refined isotropically in the final cycles of least-squares refinement. All the hydrogen atoms were refined using the riding model, except for the hydroxo hydrogen, which was allowed to vary freely with only the bond length constraint O–H = 0.85 ± 0.02 \AA . The last least-squares cycle was calculated with 347 parameters and all of the 3707 unique reflections. The weighting function used was $w^{-1} = \sigma^2(F_o^2) + (0.0600P)^2$, where $P = (F_o^2 + 2F_c^2)/3$. The maximum shift/ σ ratio was 0.149. In the last difference map the deepest hole was $-1.583 e/\text{\AA}^3$ and the highest peak was $1.221 e/\text{\AA}^3$ (within 1 \AA from Re(1)).

[NEt₄][Re₃(μ_3 -OMe)(μ -OMe)₃(CO)₉] (6). Single colorless crystals of **6** were grown by layering a solution of the compound in CH_2Cl_2 with hexane. The number of data used for structure

solution and refinement was 4598 ($I > 2.0\sigma(I)$). The structure was solved by the heavy-atom method. All non-hydrogen atoms were refined anisotropically by the full-matrix least-squares method (on F^2). Hydrogen atoms were introduced in calculated positions and refined isotropically (riding model) in the final cycles of least-squares refinement. The last least-squares cycle was calculated with 343 parameters and all of the 5357 unique reflections. The weighting function used was $w^{-1} = \sigma^2(F_o^2) + (0.0400P)^2$, where $P = (F_o^2 + 2F_c^2)/3$. The maximum shift/ σ ratio was 0.002. In the last difference map, the deepest hole was $-1.405 e/\text{\AA}^3$ and the highest peak was $0.880 e/\text{\AA}^3$.

Acknowledgment. We thank the National University of Singapore (NUS) (Grant No. RP 950695), the National Institute of Education, Nanyang Technological University (Grant No. RP 15/95 YYK), and the Academia Sinica, Taipei, for financial support. Technical assistance from the staff of the NMR Laboratory, Department of Chemistry, NUS is acknowledged. C.H.J. is grateful to NUS for a scholarship award.

Supporting Information Available: Text giving the details of X-ray structural analyses and tables of crystallographic data, refined atomic coordinates and isotropic thermal parameters, anisotropic thermal parameters, and bond lengths and angles (26 pages). Ordering information is given on any current masthead page.

OM970614L